JOURNAL OF BACTERIOLOGY, Dec. 1997, p. 7631–7637 Vol. 179, No. 24
0021-9193/97/$04.00+0

The D-Allose Operon of *Escherichia coli* K-12

CHANGHOON KIM, SUKGIL SONG, AND CHANKYU PARK*

Department of Biological Sciences, Korea Advanced Institute of Science and Technology, Yusong-Ku, Taejon, Korea

Received 7 April 1997/Accepted 1 October 1997

***Escherichia coli* K-12 can utilize D-allose, an all-*cis* hexose, as a sole carbon source. The operon responsible for D-allose metabolism was localized at 92.8 min of the *E. coli* linkage map. It consists of six genes, *alsRBACEK*, which are inducible by D-allose and are under the control of the repressor gene *alsR*. This operon is also subject to catabolite repression. Three genes, *alsB*, *alsA*, and *alsC*, appear to be necessary for transport of D-allose. D-Allose-binding protein, encoded by *alsB*, is a periplasmic protein that has an affinity for D-allose, with a K_d of 0.33 μM. As was found for other binding-protein-mediated ABC transporters, the allose transport system includes an ATP-binding component (AlsA) and a transmembrane protein (AlsC). It was found that AlsE (a putative D-allulose-6-phosphate 3-epimerase), but not AlsK (a putative D-allose kinase), is necessary for allose metabolism. During this study, we observed that the D-allose transporter is partially responsible for the low-affinity transport of D-ribose and that strain W3110, an *E. coli* prototroph, has a defect in the transport of D-allose mediated by the allose permease.**

D-Allose, an all-*cis* hexose, is utilized by *Aerobacter aerogenes*, in which the compound is converted to fructose-6-phosphate by inducible enzymes via D-allose-6-phosphate and D-allulose-6-phosphate intermediates (9, 19). *Salmonella typhimurium* LT2 and perhaps some *Escherichia coli* K-12 strains are unable to metabolize D-allose (10), but the metabolism of the sugar was not systematically studied in other bacteria. Hamster fibroblasts form D-allose-6-phosphate from D-allose, indicating that the sugar is transported and internally converted without further metabolism (33).

D-Allose has been used as an analog of D-ribose (all-*cis* pentose), since it binds to ribose-binding protein (RBP) with low affinity (1,000 times less), which is sufficient to elicit chemotaxis (1, 32). A similarity between the two sugars is apparent since they differ only in the fifth positions of their pyranose forms (1) (Fig. 1). The gene (*rbsB*) for RBP is a part of the *rbs* operon, which is located at 84 min and encodes a high-affinity transporter for D-ribose, consisting of RbsDAC proteins. Although the high-affinity system is primarily responsible for uptake of this sugar, it has been assumed that a secondary or low-affinity transporter exists, since a strain that lacks most *rbs* genes, but carries *rbsK* for ribokinase, still grows on D-ribose (14, 16). However, no information is currently available for the putative secondary transport system (15). Inside the cell, D-ribose is converted by ribokinase to ribose-5-phosphate, which is an essential compound of cellular anabolism. The compound serves as the substrate for the synthesis of phosphoribosyl diphosphate, a precursor for the biosynthesis of nucleotides and the amino acids histidine and tryptophan (30). Thus, the strain with a mutation in *rpiA*, the gene which encodes D-ribose phosphate isomerase, requires ribose for growth since ribose-5-phosphate cannot be generated from other sugars (13, 28).

A study on *rpiA* gene led to a discovery of two linked genes at 92.8 min, *rpiR* and *rpiB* (30), which are suggested in this study to be involved in allose utilization. The ribose auxotrophy resulting from a defect in *rpiA* was relieved either by an *rpiR* mutation or by an overproduction of RpiB. The RpiB protein has an enzymatic activity similar to that of RpiA. Nevertheless, they do not show amino acid sequence similarity. The inducibility of *rpiB* by D-ribose, however, has not been clearly established, although *rpiR* apparently serves as a regulatory gene. In the same region, an *rpe* (encoding D-ribulose-5-phosphate 3-epimerase) homolog of *Alcaligenes eutrophus* pHG1 was discovered by *E. coli* genome sequencing and predicted as an open reading frame, *f231* (3). Recently, a gene which appears to be involved in the epimerization of D-ribulose-5-phosphate to produce D-xylulose-5-phosphate was found and mapped at 74 min of the *E. coli* chromosome (17, 31). This gene, an *E. coli* version of *rpe*, is more similar to the *rpe* gene of *A. eutrophus* pHG1 than to *f231*, with 63 and 36% identities, respectively (21).

Here, we describe the complete operon, located at 92.8 min of the *E. coli* linkage map, that is primarily responsible for D-allose transport and metabolism and that, in addition, appears to be involved in the transport of D-ribose at low affinity.

MATERIALS AND METHODS

Strains and plasmids. Strains used in this study are derivatives of *E. coli* K-12 and are listed in Table 1. The mutations Δ*rbs*(*D-R*)::*spc*, *malE*::Tn*10*, and *acs*::*aph* were from OW1ΔRD, LS311, and LS300, respectively. Minicell-producing strain CP1012, lacking the repressor gene for D-allose, was made by introducing Δ*als*(*R* to *K*)::*tet* into HB290. Plasmid pTS105 has a large deletion of *rbsB* in pAI12 that is not polar on the expression of downstream *rbsK*. Plasmid pSK131 (3.65 kb) consists of a fragment of the transposase gene (1.24 kb of the *Pvu*II/*Hpa*I fragment from λ::Tn*phoA′-1*), part of multicloning site [25 bp of the *Sma*I/*Xba*I fragment from pGEM-7Zf(+), Promega], and the *Xba*I/*Pvu*II fragment (2.40 kb) of the replicon which is derived from pBluescript II SK(+) (2.96 kb; Stratagene) after deletion of the *Kpn*I/*Nae*I fragment (327 bp with the COOH-terminal LacZα) and filling in of the *Eco*RI site at the multicloning site. The transposon-hopping phages λ::Tn*phoA′-1* and λ::Tn*phoA′-2* were obtained from B. Wanner (34), and λRS45 was obtained from R. W. Simons (27).

Chemicals. D-Allose and D-ribose were purchased from Sigma Chemical Co. Restriction enzymes and [^{35}S]methionine (1,000 Ci/mmol) were purchased from Boehringer Mannheim and Amersham Corp., respectively. Other chemicals used were reagent grade.

Cell growth and minicell preparation. H1 minimal medium (23) containing appropriate concentrations of sugars was used in cell growth experiments. Cells were cultured in 0.4% glycerol H1 minimal medium at 37°C and were used as an inoculum. Growth in 0.2% D-allose medium was at 37°C, with shaking at 120 rpm in a flask filled with about 10% volume of H1 minimal medium. Small aliquots from cultures with 0.2% D-allose were taken every 2 h during growth to measure the optical density at 600 nm.

To detect proteins expressed from a cloned DNA fragment, a strain with a plasmid was grown to early stationary phase in LB medium containing appropriate antibiotics, and minicells were prepared as described previously (6). The

* Corresponding author. Phone: 82-42-869-4019. Fax: 82-42-869-2610. E-mail: ckpark@hanbit.kaist.ac.kr.

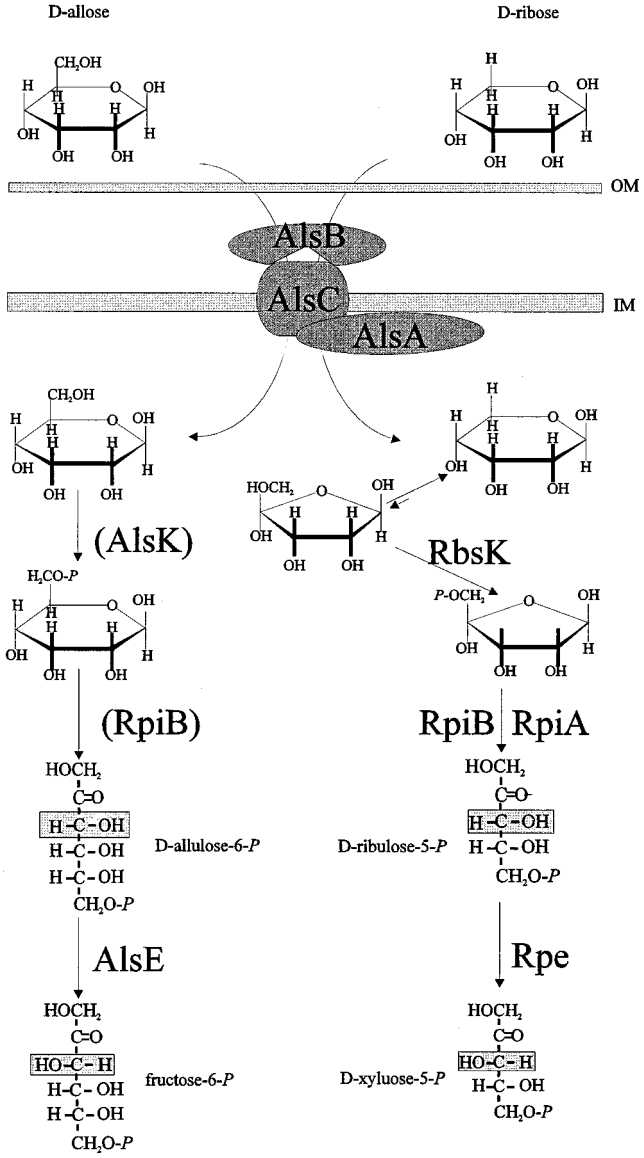

FIG. 1. Schematic illustration of the proposed functions of Als components in the transport and metabolism of D-allose. Names of the gene products are as in Table 4. D-Allose and D-ribose appear to be transported as analogous structures by the permease. An equilibrium of D-ribose is shifted toward pyranose (80%) in solution and is phosphorylated as a furanose by RbsK. The structure of D-ribose (outside) is shown as a pyranose since it is the form found in the crystal structure of RBP. AlsK and RpiB are shown in parentheses because they were demonstrated to be dispensable (see Results). RpiA is ribose-5-phosphate isomerase whose activity can be replaced by RpiB. RpiB is also postulated to be an allose-6-phosphate isomerase because it is a part of the operon and under the control of AlsR. The positions of epimerizations are shaded. Abbreviations: *P*, phosphoryl group; OM, outer membrane; IM, inner membrane.

plasmid-coded proteins in minicells were labeled with [^{35}S]methionine, separated by electrophoresis on sodium dodecyl sulfate–12% polyacrylamide gels, and subjected to autoradiography.

DNA manipulation. DNA preparation and recombinant DNA techniques followed standard procedures (26). DNA sequencing was performed by using a kit from Amersham Corp., with four primers designed to cover the whole region of the *alsR* gene. To determine the site of a transposon insertion obtained in vivo, we developed a strategy (29) in which plasmid pSK131 containing the transposase gene was first integrated into the chromosomal transposase gene by homologous recombination; the same plasmid with an extra chromosomal region was then recovered by preparing the chromosomal DNA and digesting it with an appropriate restriction enzyme before ligation. Integration of the plasmid was facilitated in *polA*(Ts) background, which enabled the formation of a cointegrate through selection of the plasmid marker under nonpermissive conditions since the PolA protein is necessary for the episomal maintenance of the plasmid (23). The order *′tnp*(N-terminus)-*mcs-bla-ori′* of markers on the plasmid was established by DNA manipulation, so that digestion of the cointegrate with one of the enzymes recognizing *mcs* would allow the plasmid to acquire the chromosomal fragment that was bordered by the NH_2-terminal side of the *tnp* gene. The *als* genes and the mutations in *alsR* were obtained in this manner from plasmids integrated into *zjc-1*::Tn*phoA′*-1. These are pSK185 (*Kpn*I digestion) and the parental plasmids for pHN200 to pHN204 (all with *Bgl*II/*Bam*HI digestions). The *Bst*EII fragment of pSK185, containing most of the *als* genes, was substituted with the *Eco*RI/*Ava*I fragment (*tet*) of pBR322 by filling in the ends with Klenow enzyme and blunt-end ligation, resulting in pHN208. The 10-kb *Eco*RI fragment of pSK185 was subcloned into the *Eco*RI site of pBR328 to make low-copy-number plasmid pHN205. From pHN205, plasmids pHN212 (*Ava*I deletion), pHN213 (*Hin*dIII deletion), pHN214 (*Hpa*I deletion), and pHN219 (*Not*I/*Bam*HI deletion) were made. Plasmid pHN228 was generated by removing the *Bgl*II/*Acc*I fragment from pHN219 with enzyme treatments. This plasmid has the intact downstream genes *alsA* and *alsC*. Plasmid pHN217 was made by replacing the 1.47-kb *Eco*RI/*Bss*HII fragment of pHN213 with that of pHN201.

To construct transcriptional fusions in vitro, the *Eco*RI/*Bgl*II fragment was divided into two parts by PCR using four primers. For cloning the 5′ 1,059-bp fragment, two primers, 5′-CAGACCGCGCGAATTCCGGC-3′, for synthesizing downward from the *Eco*RI site in *rpiB* (Fig. 2), and 5′-GGAGGATCCCTCCG GCACCGTACA-3′, for synthesizing upward from 488 bp downstream of the *alsR* translation start with a *Bam*HI end, were used. For the 3′ 795-bp fragment, primers 5′-GGGGAATTCTATCAGGGCAGACAGCG-3′, recognizing 445 downstream of the *alsR* translation start site with an *Eco*RI end, and 5′-GGAT AATGGAGCGAACCGCA-3′, for synthesizing upward from 276 bp downstream of the *alsB* translation start, were used. The two DNA fragments amplified by using the LA-Taq polymerase (Takara Shuzo), each digested with *Eco*RI/*Bam*HI and with *Eco*RI/*Bgl*II, were cloned into the *Eco*RI/*Bam*HI site of pRS551 (27), yielding pHN265 and pHN266, respectively. Plasmid pRS551 has the *lac* gene on the *Bam*HI side. They were transferred to λRS45 and lysogenized into appropriate hosts (see below). Single-copy λ prophages were confirmed by PCR with three primers recognizing *E. coli attB*, λ *attP*, and λ *int* genes (24).

Genetic manipulation. P1 transduction (18), *polA*(Ts) integration (23), and transposon mutagenesis (34) were conducted as previously described. The spontaneous mutations *alsR101* through *alsR106*, giving rise to the Rib^e phenotype (see Results) were selected from CP1007/pTS105 on H1 minimal plates containing 0.2% D-ribose and appropriate antibiotics. The transposon-hopping phages λ::Tn*phoA′-1* and λ::Tn*phoA′-2* were used for insertion mutagenesis as described previously (34). Transposon insertions that abolish the Rib^e phenotype of CP1008/pTS105 were isolated at frequencies of 8/4,000 for Tn*phoA′-1* and 4/4,000 for Tn*phoA′-2* by replica plating; 5 of 14 insertions were Lac$^+$, with various degrees of β-galactosidase expression.

Spontaneous mutations in the *alsR* gene were tagged with nearby insertions by transducing CP1007/pTS105 with the P1 lysate prepared from about 10,000 independent insertions in CP1008/pTS105. Two candidates, *zjc-1*::Tn*phoA′-1* and *zjc-2*::Tn*phoA′-1*, were tested for linkage to the spontaneous mutations of *alsR*, which exhibited 97 and 30% cotransduction frequencies, respectively. The *zjc-1*::Tn*phoA′-1* insertion was further used for cloning *alsR* mutations in *polA*(Ts) strain (CP367). First, the insertion was separated from the *alsR106* point mutation by transferring it to CP1007/pTS105. The resulting *alsR*$^+$ *zjc-1*::Tn*phoA′-1* strain was then crossed with the strains containing other *alsR* mutations. The mutations tagged with *zjc-1*::Tn*phoA′-1* were moved to the *polA*(Ts) strain and were cloned by using the strategy described for DNA manipulation.

To generate an operon-wide deletion in *als* genes, plasmid pHN208, containing the *tet* gene instead of the whole *als* operon (contained in the *Bst*EII fragments as shown in Fig. 2), was transformed into the *polA*(Ts) strain. After integration of the plasmid into the chromosome at 42°C, the plasmid portion was cured. This resulted in two different kinds of recombinants, Tet^r Amp^s and Tet^s Amp^s, since the pHN208 plasmid provides homologies on both sides of the *tet* gene. The Δ*als*(*R-K*)::*tet* insertion obtained was transferred to CP1008/pTS105 to confirm that the *als* region was inactivated, and the insertion was also used to generate the CP1010 strain.

The strains with single-copy transcriptional fusion were made as described by Simons and Kleckner (27). CP1010 was transformed with pHN265 and pHN266, and the plasmid-borne fusions were transferred to λ by infecting them with λRS45, yielding λHN265 and λHN266, respectively. CP1010 strain was then lysogenized with λHN265 (CP1031) and λHN266 (CP1032), and CP1007 was lysogenized with λHN265 (CP1033) and λHN266 (CP1034).

Measurement of K_d by fluorescence spectroscopy. Allose-binding protein (ALBP or AlsB) was purified (>95% homogeneity) from cells grown in LB medium by osmotic shock (22) and DEAE-Sepharose/carboxymethyl-Sepharose ion-exchange chromatography. About 0.5 μM ALBP was used for fluorescence measurement, showing an emission maximum of 338 nm when excited at 295 nm. When 1 mM D-allose was added in excess, the maximum was blue shifted to 327 nm in 50 mM potassium phosphate buffer at pH 7.5. We developed here the following relationship based on the single binding kinetics for ligand (7) in order to calculate the dissociation constant (K_d) of ALBP from the emission spectra. The degree of emission measured from intermediate concentrations of D-allose

TABLE 1. Strains and plasmids used in this study

Strain or plasmid	Genotype	Reference or source
Strains		
CP367	*leu thr his thi rpsL lacY xyl ara tonA tsx polA*(Ts)	23
CP1007	MC4100 Δ*rbs*(*D–R*)::*spc*	This work
CP1008	CP1007 *alsR106*	This work
CP1009	CP1008 *alsB3*::Tn*phoA′-1* (Kan^r)	This work
CP1010	CP1008 Δ*als*(*R–K*)::*tet*	This work
CP1011	MC4100 Δ*als*(*R–K*)::*tet*	This work
CP1012	HB290 Δ*als*(*R–K*)::*tet*	This work
CP1013	W3110 Δ*rbsB4*	This work
CP1031	CP1010 λHN265	This work
CP1032	CP1010 λHN266	This work
CP1033	CP1007 λHN265	This work
CP1034	CP1007 λHN266	This work
HB290	*minA minB rpsL*	G. L. Hazelbauer
LS300	CP367 *acs*::*aph*	D. Lee
LS311	W3110 *cfs malE*::Tn*10*	D. Lee
MC4100	F$^-$ Δ(*argF-lac*)*U169 rpsL relL flhD deoC ptsF rbsR*	11
MG1655	Wild type	F. A. Blattner
OW1ΔRD	*leu thr his thi rpsL lacY xyl ara tonA tsx* Δ*rbs*(*D–R*)::*spc*	A. Binnie
W3110	F$^-$ prototroph	2
Plasmids		
pAI12	pACYC184 *rbsB*$^+$*C*$^+$*K*$^+$	A. Iida
pBluescript II SK(+)	Ap^r	Stratagene
pBR328	Ap^r Cm^r Tc^r	Boehringer Mannheim
pHN200	pSK131 *rpiB*$^+$ *alsR106* (ΔT at bp 822 to 828 of *alsR*)	This work
pHN201	pSK131 *rpiB*$^+$ *alsR*$^+$	This work
pHN202	pSK131 *rpiB*$^+$ *alsR102*[a] (A227E)	This work
pHN204	pSK131 *rpiB*$^+$ *alsO1* (or *alsR104* with ΔT at bp −50 to −44 of *alsR*)	This work
pHN205	pBR328 *alsR106B*$^+$*A*$^+$*C*$^+$*E*$^+$*K*$^+$	This work
pHN208	pSK185 *rpiB*$^+$ Δ*als*(*R–K*)::*tet*	This work
pHN212	pHN205 *alsR106B*$^+$*A*$^+$	This work
pHN213	pHN205 *alsR106*	This work
pHN214	pHN205 *alsR106B*$^+$*A*$^+$*C*$^+$*E*$^+$	This work
pHN217	pHN213 *alsR*$^+$	This work
pHN219	pHN205 *alsR106B*$^+$*A*$^+$*C*$^+$	This work
pHN228	pHN219 *alsR106*Δ*BA*$^+$*C*$^+$	This work
pHN265	pRS551 *′rpiB-alsR′*	This work
pHN266	pRS551 *′alsR-alsB′*	This work
pRS551	Ap^r Kan^r *lacZYA*	27
pSK131	pBluescript II SK(+) *tnp′*	This work
pSK185	pSK131 *rpiB*$^+$ *alsR106B*$^+$*A*$^+$*C*$^+$*E*$^+$*K*$^+$	This work
pTS105	pAI12 Δ*rbsB4*	T. Song

[a] *alsR103* has the same mutational change in amino acid residue.

can be expressed as a linear combination of spectra, $F(x,\lambda)$, from allose-free and allose-bound ALBPs:

$$F(x,\lambda) = A(x) \cdot H(\lambda) + B(x) \cdot G(\lambda) \quad (1)$$

where $A(x) + B(x) = 1.0$, $A(x)$ is the fraction of allose-bound ALBP, $B(x)$ is the fraction of allose-free ALBP, $H(\lambda)$ is the spectrum of allose-bound ALBP in 1 mM D-allose, and $G(\lambda)$ is the spectrum of free ALBP. In addition, the ligand-bound fraction is obtained from the single-binding kinetics (7):

$$B_b = B_0 \cdot L/(K_d + L) \quad (2)$$

where B_b, B_0, and L are the concentrations of ligand-bound protein, total protein, and free ligand, respectively. Since the concentration of free ligand was not known, we used the concentration of total ligand (x) instead. By replacing L with $x - B_b$ in equation 2 and rearranging the equation for the variable B_b, we obtained the following quadratic equation:

$$B_b^2 - (B_0 + K_d + x) \cdot B_b + B_0 \cdot x = 0 \quad (3)$$

Meanwhile, the following equation was derived from the relationship $A(x) = B_b/B_0$ and from B_b expressed as a function of x as in equation 3:

$$A(x) = [K_d + x + B_0 - Sqrt\ (K_d^2 + x^2 + B_0^2 + 2K_d \cdot x + 2B_0 \cdot K_d - 2B_0 \cdot x)]/(2B_0) \quad (4)$$

The $A(x)$ and $B(x)$ values are obtained by fitting the observed spectra to equation 1. The sum of $A(x)$ and $B(x)$ was nearly a unit value within 2% deviation. Finally, K_d and B_0 were obtained from the nonlinear regression analysis of $A(x)$ in equation 4.

RESULTS

Screening for a mutation affecting ribose growth. *E. coli* cells are able to grow on D-ribose, albeit less efficiently, even when there is a defect in the high-affinity uptake (K_m of 0.91 μM [5]). Thus, the presence of a low-affinity transporter has been implicated. The low-affinity system seems to share the D-ribose kinase (*rbsK* gene product) with the high-affinity system for its metabolism of sugar (16). By introducing a deletion Δ*rbs*(*D-R*)::*spc*, we constructed the strain (CP1007) lacking all of the *rbs* components except the *rbsK* gene, which is supplied by plasmid pTS105. This strain (CP1007/pTS105) allowed us to screen for a secondary mutation that affects D-ribose utilization (Table 2).

Spontaneous mutant derivatives of CP1007/pTS105 that exhibited an enhanced growth on D-ribose minimal plates were

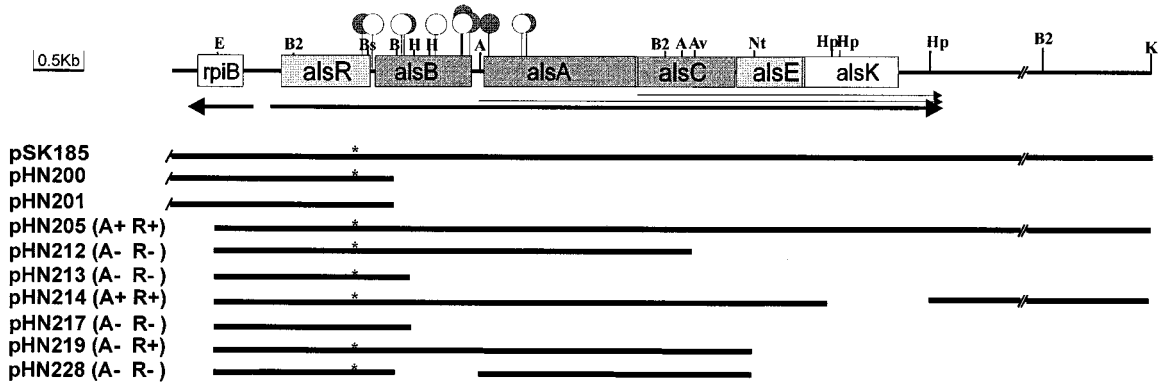

FIG. 2. Genetic organization and plasmid maps. The dark-shaded boxes are the components of D-allose permease: AlsB, periplasmic D-allose-binding protein; AlsA and AlsC, membrane-associated components. The negative regulator AlsR and the putative D-allulose-6-phosphate 3-epimerase (AlsE) are lightly shaded. The circles represent transposon insertions, either a Lac^+ transcriptional fusion (open) or not (filled). Each number in parentheses below represents the position of the base flanking the insertion site, which is counted from the translational start, upstream (−) or downstream (+) of a corresponding gene: *alsR1*::Tn*phoA′-1* (*alsR*+850), *alsR′B1*::Tn*phoA′-1* (*alsB*−23), *alsB1*::Tn*phoA′-1* (*alsB*+276), *alsB2*::Tn*phoA′-1* (*alsB*+922), *alsB3*::Tn*phoA′-1* (*alsB*+412), *alsB4*::Tn*phoA′-1* (*alsB*+843), *alsB5*::Tn*phoA′-1* (*alsB*+834), *alsB6*::Tn*phoA′-2* (*alsB*+857), *alsB7*::Tn*phoA′-2* (*alsB*+252), *alsA1*::Tn*phoA′-1* (*alsA*+421), *alsA2*::Tn*phoA′-2* (*alsA*+378), and *alsA3*::Tn*phoA′-2* (*alsA*+49). The arrows beneath the map show the transcriptions predicted (3, 4). Two internal promoters in the middle of the rightward operon do not seem to be functional based on our complementation data (see Results for details). Complementation for ribose (R) or D-allose (A) growth is designated in parentheses. The presence of the *alsR106* mutation is shown with an asterisk. Restriction sites used to generate the plasmids: A, *Acc*I; Av, *Ava*I; B, *Bgl*II; B2, *Bst*EII; Bs, *Bss*HII; E, *Eco*RI; H, *Hin*dIII; Hp, *Hpa*I; K, *Kpn*I; Nt, *Not*I.

obtained at a frequency of 10^{-6} to 10^{-7}. The phenotype, caused by the mutation designated here Rib^e (enhanced) (Table 2), is intermediate between the Rib^+ phenotype that is conferred by the functional high-affinity transporter and the Rib^- phenotype that is observed in a strain lacking the high-affinity permease and conferred by the so-called low-affinity transporter. We characterized six independent mutations giving rise to the Rib^e phenotypes that are closely linked to a particular locus of the *E. coli* linkage map and were named *alsR101* through *alsR106* (see below). To determine their genetic locations, two nearby transposon insertions, *zjc-1*::Tn*phoA′-1* and *zjc-2*::Tn*phoA′-1*, were obtained and used to map the mutations to 92.8 min. We suspected that the mutations might occur in a regulatory gene, since their consequence was a gain of function arising at high frequency.

Further attempts to isolate a structural gene mutation restoring Rib^- from Rib^e phenotype from the *alsR106* strain (CP1008/pTS105) yielded other class of insertional mutations in the vicinity of *alsR*. One insertion (*alsR′B1*::Tn*phoA′-1*) was found in the intercistronic region between *alsR* and *alsB*, and others were found in three open reading frames, *alsR*, *alsB*, and *alsA*, as named in Fig. 2.

To analyze the insertions, flanking regions of the insertion sites were cloned and sequenced by using plasmid pSK131, containing the terminal segment of the transposon which facilitates homologous recombination between the plasmid and chromosome in the *polA*(Ts) strain (23). An inserted plasmid was recovered by restriction digestion, ligation, and transformation into a host strain (see Materials and Methods for details). The insertion boundaries were found in the open reading frames constituting an operon whose sequence was determined by the *E. coli* genome project (3, 4). The locations and orientations of insertions are shown in Fig. 2 with their assigned names, based on the sequence homologies and also on functional characterizations described below.

The point mutations showing Rib^e phenotypes were found in the reading frame or in the promoter region of *alsR*; the changes are summarized in Table 3. The *alsR106* deletion does not seem to cause any significant polar effect on the expression of downstream genes. Since the *alsO1* mutation is *cis* dominant and the $alsR^+$ gene in this background can complement the *alsR106* point mutation (Table 3), it is very likely that the *alsO1* mutation lies in the operator region to which AlsR binds.

***als* genes and their products.** Open reading frames in the predicted operon are oriented in the same direction (Fig. 2). The proteins encoded have alternative names in the Swiss-Prot database with annotations for homologous proteins, as shown in Table 4. It was reported that AlsK has similarity to XylR of *Bacillus subtilis* (23.6% identity [3]). In our analysis, however, AlsK is more similar to glucokinase of *Streptomyces coelicolor* (25.9%) than to XylR of *B. subtilis* (19.1%). *alsR* has been found as *rpiR* and was proposed to encode a repressor for the *rpiB* gene, which is transcribed in the opposite direction from *alsR* (30). Since our data clearly indicate that the genes in this operon are involved in the metabolism of D-allose (see below), they were renamed *alsR*, *alsB*, *alsA*, *alsC*, *alsE*, and *alsK* (Table 4). The *alsB*, *alsA*, and *alsE* products were detected in a minicell labeled with [^{35}S]methionine with estimated sizes of 30.1, 60, and 27.8 kDa, respectively (data not shown). The AlsB protein has a signal sequence and was released with other

TABLE 2. Sugar utilization in various mutants

Strain	Genotype		Growth[a]	
	als	*rbs*	Allose	Ribose
CP1007	+	Δ(*D–R*)	++	−
CP1007/pTS105	+	Δ(*D–R*) K^+	++	+/−[b]
CP1008/pTS105	*R106*	Δ(*D–R*) K^+	++	+[c]
CP1009/pTS105	*R106*/*B3*::Tn*phoA′-1*	Δ(*D–R*) K^+	−	+/−
CP1010	Δ(*R–K*)	Δ(*D–R*)	−	−
CP1011	Δ(*R–K*)	+	−	++
CP1013	*C*	Δ*B*	+/−	+/−
MC4100	+	+	++	++
MG1655	+	+	++	++
W3110	*C*	+	+/−	++

[a] Measured on H1 minimal plates with 0.2% of sugar. Symbols represent relative levels of growth.
[b] Background growth was detected due to a nonspecific transport.
[c] Rib^e phenotype.

TABLE 3. Properties of spontaneous mutations obtained in *alsR*

alsR allele[a]	Mutational change	Merodiploid with *alsR106*[b]		Comment
		Plasmid	*alsB*::*lacZ* activity[c]	
None	None	pSK131	1,307	Control vector
alsO1	ΔT at bp −50 to −44[d]	pHN204	35	Operator mutation (=*alsR104*)
alsR$^+$	Wild type	pHN201	45	
alsR102/*103*	A227E	pHN202	1,204	Missense mutation
alsR106	ΔT at bp 822 to 828[e]	pHN200	958	Nonpolar deletion

[a] Carried on a plasmid.
[b] Tests were done in the CP1009 (*alsR106*) background.
[c] The β-galactosidase assay was performed in tryptone broth, and activities are shown in Miller units.
[d] The base pairs numbered from the translation initiation site comprise seven repeated T's.
[e] The region comprises 7 T's in the reading frame. The deletion does not cause polarity to the downstream genes, perhaps because it does not result in an immediate termination.

secreted proteins by osmotic shock (not shown), indicating a periplasmic binding protein.

Organization and regulation of the *als* operon. The transcriptional fusions (Fig. 2) in the *als* operon were Lac$^+$ in their original background but became repressed when AlsR was supplied from a plasmid, implying that the AlsR is a negative regulator for the *als* operon (data not shown). It was suggested that the *als* genes are transcribed as a monocistronic message from the promoter located just upstream of *alsR* (4). A failure to isolate an insertional mutation with Rib^e in the *als* region (29a) raises the possibility that the insertion would not allow the expression of downstream genes necessary for supporting ribose growth. Indeed, the *alsR1*::Tn*phoA′-1* insertion abolished the phenotype of *alsR106*, indicating that the insertion is polar to the downstream genes. In addition, *alsO1* mutation when supplied on a plasmid is phenotypically Rib^e and represses the chromosomal *lacZ* fusion (*alsB3*::Tn*phoA′-1*). These results strongly suggest that a negative regulator AlsR is coordinately expressed with the downstream structural genes presumably as a single *alsRBACEK* operon (Table 4). Although internal promoters were suggested between the *alsB* and *alsA* genes and within *alsC* gene (3, 4) (Fig. 2), they do not seem to be functional because pHN219 (*alsR106B*$^+$*A*$^+$*C*$^+$) could not complement *alsB3*::Tn*phoA′-1* polar insertion in allose utilization that requires the functional AlsE protein (see below).

The fact that *alsR* itself is regulated by allose as a first gene of the operon was further confirmed by examining an inducibility of the two transcriptional fusions, one containing the promoter and the beginning of *alsR* gene ('*rpiB-alsR*') and the other containing the portions of *alsR* and *alsB* ('*alsR-alsB*'; see Materials and Methods). The fusions were tested after being lysogenized into a single copy. The '*rpiB-alsR*' fusion is repressible by AlsR and inducible by allose, not by ribose, whereas the '*alsR-alsB*' fusion does not exert any transcriptional activity (Fig. 3). The induction by allose is subject to catabolite repression, which again confirms that *alsR* is coregulated as part of the operon with *alsB* and other downstream genes.

Als components in transport and metabolism. Although the operon was initially characterized as enhancing D-ribose growth, we presumed that there might be a high-affinity substrate for the *als* system since a mutational derepression of the operon could provide an activity of the secondary transporter for ribose. D-Allose has been regarded as a nonmetabolizable analog of D-ribose. However, only D-allose among tested sugars, including D-xylose and 2-deoxyribose, which are structurally related to D-ribose, showed a significant difference in supporting the growth of the *als*$^+$ (MC4100) and the *als*-null (CP1011) strains. We examined growth on D-allose in several other *E. coli* strains, including MG1655 (wild type) and W3110. MG1655 and MC4100 grew as well on 0.2% D-allose plates as on 0.2% D-ribose plates, whereas W3110 showed poor growth on 0.2% D-allose (Table 2). The involvement of the *als* operon in utilizing D-allose was further confirmed either by deleting the whole region with Δ*als*(*R-K*)::*tet* as in CP1010 (a negative control) or by introducing plasmid pHN205, containing the whole region of *als* operon, into the CP1010 strain derived from MC4100. The doubling times in D-allose minimal medium were measured for MC4100 (110 to 120 min), W3110 (350 to 400 min), and CP1007 (Δ*rbs*) (110 min). Strains CP1010 (Δ*rbs* Δ*als*) and CP1011 (*rbs*$^+$ Δ*als*) did not show any growth.

We made several deletions of pHN205 to characterize components that are necessary for growth on D-allose or D-ribose (Fig. 2). pHN214, with a deletion in *alsK*, supports growth on allose in a Δ*als* background, indicating that *alsK* is not essen-

TABLE 4. Properties of the *als* components

Name	Proposed function	Hypothetical protein (ORF[a])	Similarity[b] (%)	Sequence characteristics
rpiB	Allose-6-P isomerase	YjcZ (*o143*)	Ribose-5-P isomerase	
alsR	Repressor for *als* and *rpiB*	YjcY (*f307*)		Helix-turn-helix
alsB	Allose-binding protein	YjcX (*f311*)	Ribose-binding protein (RbsB) (34.1)	Signal peptide
alsA	ABC protein (transport)	YjcW (*f510*)	ABC protein for transport (MglA) (40.9)	ATP-binding cassette
alsC	Transport component	YjcV (*f326*)	RbsC (membrane component) (39.6)	8 transmembrane peptides
alsE	Allulose-6-P 3-epimerase	YjcU (*f231*)	Rpe[c] (ribulose-5-P 3-epimerase) (33.3)	
alsK	Allose kinase	YjcT (*f309*)	XylR[d] (19.1) or glucokinase[e] (25.9)	Helix-turn-helix

[a] Open reading frame as designated in the Swiss-Prot database (25).
[b] Based on method of Myers and Miller (21).
[c] From *A. eutrophus* pHG1.
[d] XylR of *B. subtilis* (12).
[e] Glucokinase of *S. coelicolor.*

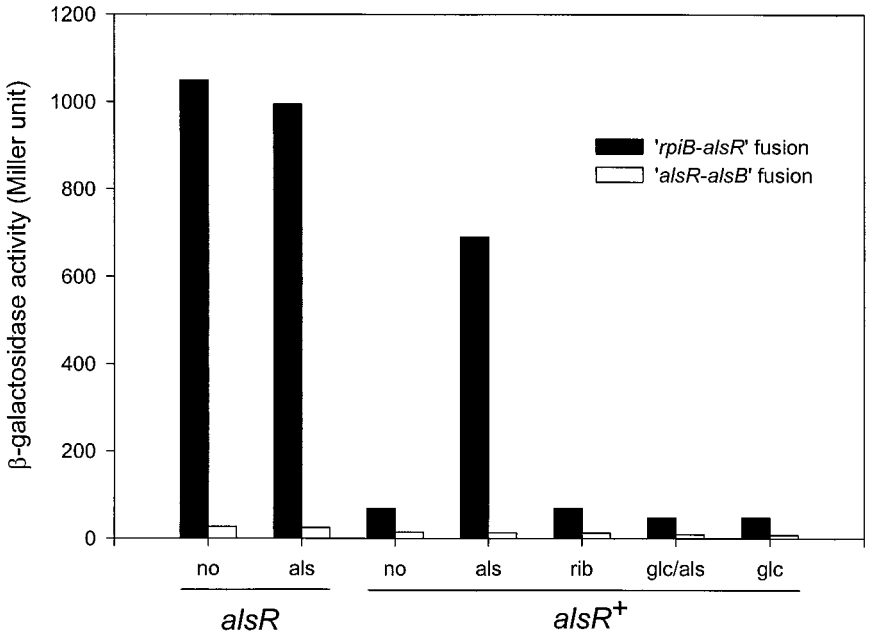

FIG. 3. Regulatory characteristics of the *als* operon. Cells were grown in H1 minimal medium with 0.4% glycerol to an A_{600} of about 0.1, the effectors were added, and the cells were further incubated for 2 h. β-Galactosidase activity was measured as described by Miller (18). The strains used, CP1031 (*alsR 'rpiB-alsR'*), CP1032 (*alsR 'alsR-alsB'*), CP1033 (*alsR*$^+$ *'rpiB-alsR'*), and CP1034 (*alsR*$^+$ *'alsR-alsB'*), are lysogens. Effectors: no, none; als, 0.01% allose; rib, 0.2% ribose; glc, 0.2% glucose; glc/als, 0.01% allose plus 0.2% glucose.

tial. Plasmid pHN219, harboring *alsR106* and *alsBAC*, exhibited the same degree of complementation for D-ribose minimal growth as pHN205, whereas no complementation was observed for D-allose minimal growth. This result indicates that the presence of the *alsB*, *alsA*, and *alsC* genes is sufficient for D-ribose transport and that *alsE* is essential for D-allose metabolism. Although *alsE* is essential for D-allose metabolism as demonstrated by the complementation test, the roles of *alsK* and *rpiB* are still unclear because their defects had no effects on D-allose growth. Plasmids pHN212 (*alsC*) and pHN228 (*alsB*) could not restore the defect of D-ribose minimal growth in CP1010/pTS105. Expression of the remaining part of pHN228 was confirmed by its complementation to D-ribose growth defect in *alsA* polar insertion but not in *alsB* polar insertion. An involvement of *alsA* was similarly demonstrated in a Δ*rbs* Δ*als* background with an internal deletion made in *alsA* (most of the gene by *Bal*I/*Nru*I digestion) that did not support either allose or ribose growth without affecting the expression of downstream genes. In conclusion, all three components, *alsB*, *alsA*, and *alsC*, are required for complementation of the D-ribose growth defect, whereas *alsE* is additionally required for D-allose utilization. Furthermore, it was suggested that these three components, normally for D-allose transport, constitute an alternative ABC transporter for D-ribose.

Since strain W3110 did not grow on D-allose, we postulated that the strain may have a defect in one of the *als* genes. This possibility is consistent with the result that no *als* mutations with Rib^e phenotypes were isolated from the high-affinity negative derivative (CP1013) of W3110. The slow growth of the strain on D-allose appears to be mediated by the D-ribose permease. When we introduced plasmids pHN205, pHN212, pHN219, and pHN228 into CP1013, all except pHN212 (*alsC*) complemented the D-ribose growth defect as well as the D-allose defect. This result indicates that the *alsC* gene encoding a putative membrane component is defective in W3110.

Determination of the affinity of the allose-binding protein for allose. To demonstrate the direct binding of D-allose to ALBP, partially purified protein (Materials and Methods) was mixed with different concentrations of D-allose, and subsequent changes in intrinsic fluorescence were monitored. Since two of three tryptophans were localized in the sugar-binding cleft on the three-dimensional structure of ALBP (19a) predicted from its sequence similarity to RBP, they were used for fluorescence spectroscopy with an excitation at 295 nm. Using the property of blue shift in λ_{max} by an addition of D-allose, we obtained spectra with various degrees of allose concentrations from 0.1 to 8.0 μM. Since the spectrum at a given concentration of D-allose reflects a fractional saturation, spectra obtained from intermediate concentrations of D-allose could be fitted to equation 1 (see Materials and Methods), and the values of $A(x)$ and $B(x)$ were calculated. Subsequently, they were incorporated into equation 2 to obtain K_d and B_0. The total amount of ALBP (B_0) estimated was about 0.43 μM, and the K_d measured for D-allose was about 0.33 ± 0.016 μM, which is comparable with K_ds for other high-affinity binding proteins.

DISCUSSION

We characterized spontaneous mutations that partially compensated for a defect in high-affinity ribose transport, which were mapped at 92.8 min of the *E. coli* linkage map. The mutations inactivated *alsR* or the operator site (*alsO*) of *alsR*, to make it constitutive. Therefore, it was deduced that AlsR regulates the *als* operon, which contains genes for the transport and metabolism of D-allose. *alsR* was also reported to be a negative regulator for the *rpiB* gene coding for a secondary D-ribose-5-phosphate isomerase (30). We also generated insertion/deletion mutations of *als* structural genes, thereby assigning physiological functions for the hypothetical *als* genes predicted by the genome sequencing (3, 4).

It was demonstrated that strains MC4100 and MG1655 were capable of utilizing D-allose as a carbon source through the D-allose permease that also transports D-ribose at low affinity.

It is not surprising that allose and ribose transport systems are functionally redundant because D-ribose exists primarily as a pyranose form (80%) in solution, which is presumably responsible for interacting with the periplasmic binding protein (20) and also with the membrane components (Fig. 1). This configuration of D-ribose is structurally analogous to that of D-allose. Moreover, D-ribose can still be utilized when both the ribose and allose systems are absent (14a), suggesting that other structurally related permeases provide the remaining activity of low-affinity transport. The situation is different for other pentose transport systems, where they have their own low-affinity permeases that belong to the LacY family, e.g., XylE for D-xylose and AraE for L-arabinose. In any case, it appears that structurally related compounds share transport systems without relying on their specific low-affinity systems. It has been reported that L-arabinose is transported by the high-affinity transport system of D-galactose and that D-galactose is transported by at least six independent permeases (8).

We found that AlsE (epimerase) is essential, although AlsK (kinase) and RpiB (isomerase) are dispensable for D-allose utilization (Fig. 1). In *A. aerogenes* (9), it was shown that D-allose kinase and D-allose-6-phosphate isomerase activities are required. Our finding that only AlsE is essential may indicate that other functionally analogous enzymes substitute for the activities of D-allose kinase and D-allose-6-phosphate isomerase, although it is still possible that RpiB and AlsK play unexpected roles in D-allose metabolism. The structural similarity of hexoses may explain the cross-specificity. In *A. aerogenes*, only D-allose-6-phosphate isomerase activity was dramatically increased when D-allose was added to a culture medium, whereas the D-allose kinase activity remained to be expressed at a rather constitutive level (9), suggesting that allose kinase activity might be redundant. Since it was shown that RpiB has the activity of D-ribose-5-phosphate isomerase, we predict that RpiB also has D-allose-6-phosphate isomerase activity, based on the finding that galactose-6-phosphate isomerase can replace pentose phosphate isomerase in *Streptococcus mutans* (30). In this regard, it is of interest that D-allulose-6-phosphate 3-epimerase (AlsE) is essential even though D-ribulose-5-phosphate 3-epimerase (Rpe), similar to AlsE in primary sequence (36% identity), is already expressed. Since there are no similar steps requiring 3-epimerase activity in hexose metabolism of *E. coli*, this may explain why the AlsE function is specific, whereas that is not the case in RpiB.

ACKNOWLEDGMENTS

We thank A. Binnie and M. Hermodson for providing strains, A. Schneider for correcting the manuscript, Seungjin Kim for generating the *alsA* deletion, and S. Mowbray for modeling the structure of allose-binding protein and for reading the manuscript.

This work was supported by a grant KOSEF 96-0401-01-01-3 from the Korea Science and Engineering Foundation.

REFERENCES

1. **Aksamit, R. A., and D. E. Koshland, Jr.** 1974. Identification of the ribose binding protein as the receptor for ribose chemotaxis in *Salmonella typhimurium*. Biochemistry **13:**4473–4478.
2. **Bachman, B. J.** 1972. Pedigrees of some mutant strains of *Escherichia coli* K-12. Bacteriol. Rev. **36:**525–557.
3. **Blattner, F. R., V. Burland, G. Plunket III, H. J. Sofia, and D. L. Daniels.** 1993. Analysis of the *Escherichia coli* genome IV: DNA sequence of the region from 89.2 to 92.8 minutes. Nucleic Acids Res. **21:**5408–5417.
4. **Burland, V., G. Plunkett III, H. J. Sofia, D. L. Daniels, and F. R. Blattner.** 1995. Analysis of the *Escherichia coli* genome VI: DNA sequence of the region from 92.8 through 100 minutes. Nucleic Acids Res. **23:**2105–2119.
5. **Eym, Y., Y. Park, and C. Park.** 1996. Genetically probing the regions of ribose-binding protein involved in permease interaction. Mol. Microbiol. **21:**695–702.
6. **Frazer, A. C., and R. Curtiss III.** 1978. Production, properties and utility of bacterial minicells. Curr. Top. Microbiol. Immunol. **69:**1–84.
7. **Freifelder, D.** 1982. Physical biochemistry: applications to biochemistry and molecular biology, p. 654–684. W. H. Freeman and Company, San Francisco, Calif.
8. **Furlong, C. E.** 1987. Osmotic shock sensitive transport systems, p. 768–796. *In* F. C. Neidhardt, J. L. Ingraham, K. B. Low, B. Magasanik, M. Schaechter, and H. E. Umbarger (ed.), *Escherichia coli* and *Salmonella typhimurium*: cellular and molecular biology. ASM Press, Washington, D.C.
9. **Gibbins, L. N., and F. J. Simpson.** 1964. The incorporation of D-allose into the glycolytic pathway by *Aerobacter aerogenes*. Can. J. Microbiol. **10:**829–836.
10. **Gutnick, D., J. M. Calvo, T. Klopotwski, and B. N. Ames.** 1969. Compounds which serve as the sole source of carbon or nitrogen for *Salmonella typhimurium* LT2. J. Bacteriol. **100:**215–219.
11. **Hall, M. N., and T. J. Silhavy.** 1981. Genetic analysis of the *ompB* locus in *Escherichia coli* K-12. J. Mol. Biol. **151:**1–15.
12. **Hastrup, S.** 1988. Analysis of the *B. subtilis* xylose regulon, p. 79–84. *In* A. T. Cranesan and J. A. Hock (ed)., Genetics and biotechnology of *Bacilli*, vol. 2. Academic Press, Inc., New York, N.Y.
13. **Hove-Jensen, B., and M. Maigaard.** 1993. *Escherichia coli rpiA* gene encoding ribose phosphate isomerase A. J. Bacteriol. **175:**5628–5635.
14. **Iida, A., S. Harayama, T. Iino, and G. L. Hazelbauer.** 1984. Molecular cloning and characterization of genes required for ribose transport and utilization in *Escherichia coli* K-12. J. Bacteriol. **158:**674–682.

14a. **Kim, C., and C. Park.** Unpublished data.

15. **Lin, E. C. C.** 1987. Dissimilatory pathways for sugars, polyols, and carboxylates, p. 245–248. *In* F. C. Neidhardt, J. L. Ingraham, K. B. Low, B. Magasanik, M. Schaechter, and H. E. Umbarger (ed.), *Escherichia coli* and *Salmonella typhimurium*: cellular and molecular biology. ASM Press, Washington, D.C.
16. **Lopilato, J. E., J. L. Garwin, S. D. Emr, T. J. Silhavy, and J. R. Beckwith.** 1984. D-Ribose metabolism in *Escherichia coli* K-12: genetics, regulation, and transport. J. Bacteriol. **158:**665–673.
17. **Lyngstadaas, A., A. Löbner-Olesen, and E. Boye.** 1995. Characterization of three genes in the *dam*-containing operon of *Escherichia coli*. Mol. Gen. Genet. **247:**546–554.
18. **Miller, J. H.** 1972. Experiments in molecular genetics. Cold Spring Harbor Laboratory, Cold Spring Harbor, N.Y.
19. **Mortlock, R. P.** 1976. Catabolism of unnatural carbohydrates by microorganisms. Adv. Microbiol. Physiol. **13:**1–53.

19a. **Mowbray, S. L.** Unpublished data.

20. **Mowbray, S. L., and L. B. Cole.** 1992. 1.7 Å x-ray structure of the periplasmic ribose receptor from *Escherichia coli*. J. Mol. Biol. **225:**155–175.
21. **Myers, E. W., and W. Miller.** 1988. Optimal alignment in linear space. Comput. Appl. Biosci. **4:**11–17.
22. **Neu, H. C., and L. A. Heppel.** 1965. The release of enzymes from *Escherichia coli* by osmotic shock and during the formation of sphaeroplasts. J. Biol. Chem. **240:**3685–3692.
23. **Park, C., and G. L. Hazelbauer.** 1986. Mutations specifically affecting ligand interaction of Trg chemosensory transducer. J. Bacteriol. **167:**101–109.
24. **Powell, B. S., D. L. Court, Y. Nakamura, M. P. Rivas, and C. L. Turnbough, Jr.** 1994. Rapid confirmation of single copy lambda prophage integration by PCR. Nucleic Acids Res. **22:**5765–5766.
25. **Rudd, K. E.** 1993. Maps, genes, sequences, and computers: an *Escherichia coli* case study. ASM News **59:**335–341.
26. **Sambrook, J., E. F. Fritsch, and T. Maniatis.** 1989. Molecular cloning: a laboratory manual, 2nd ed. Cold Spring Harbor Laboratory Press, Cold Spring Harbor, N.Y.
27. **Simons, R. W., and N. Kleckner.** 1987. Improved single and multicopy lac-based cloning vectors for protein and operon fusions. Gene **53:**85–96.
28. **Skinner, A. J., and R. A. Cooper.** 1974. Genetic studies on ribose 5-phosphate isomerase mutants of *Escherichia coli* K-12. J. Bacteriol. **118:**1183–1185.
29. **Song, S., and C. Park.** 1997. Organization and regulation of the D-xylose operons in *Escherichia coli* K-12: XylR acts as a transcriptional activator. J. Bacteriol. **179:**7025–7032.

29a. **Song, S., and C. Park.** Unpublished data.

30. **Sørensen, K. I., and B. Hove-Jensen.** 1996. Ribose catabolism of *Escherichia coli*: characterization of the *rpiB* gene encoding ribose phosphate isomerase B and of the *rpiR* gene, which is involved in regulation of *rpiB* expression. J. Bacteriol. **178:**1003–1011.
31. **Sprenger, G. A.** 1995. Genetics of pentose-phosphate pathway enzymes of *Escherichia coli* K-12. Arch. Microbiol. **164:**324–330.
32. **Spudich, J. L., and D. E. Koshland, Jr.** 1975. Quantitation of the sensory response in bacterial chemotaxis. Proc. Natl. Acad. Sci. USA **72:**710–713.
33. **Ullrey, D. B., and H. M. Kalckar.** 1991. Search for cellular phosphorylation products of D-allose. Proc. Natl. Acad. Sci. USA **88:**1504–1505.
34. **Wilmes-Riesenberg, M. R., and B. L. Wanner.** 1992. Tn*phoA* and Tn*phoA′* elements for making and switching fusions for study of transcription, translation, and cell surface localization. J. Bacteriol. **174:**4558–4575.